


Thermodynamic trade-off relation for first passage time in resetting processesP. S. Pal,¹ Arnab Pal,^{2,3} Hyunggyu Park⁴,, and Jae Sung Lee¹¹*School of Physics, Korea Institute for Advanced Study, Seoul 02455, Korea*²*The Institute of Mathematical Sciences, CIT Campus, Taramani, Chennai 600113, India*³*Homi Bhabha National Institute, Training School Complex, Anushakti Nagar, Mumbai 400094, India*⁴*Quantum Universe Center, Korea Institute for Advanced Study, Seoul 02455, Korea*

(Received 3 January 2023; accepted 14 September 2023; published 9 October 2023)

Resetting is a strategy for boosting the speed of a target-searching process. Since its introduction over a decade ago, most studies have been carried out under the assumption that resetting takes place instantaneously. However, due to its irreversible nature, resetting processes incur a thermodynamic cost, which becomes infinite in the case of instantaneous resetting. Here, we take into consideration both the cost and the first passage time (FPT) required for a resetting process, in which the reset or return to the initial location is implemented using a trapping potential over a finite but random time period. An iterative generating function and a counting functional method à la Feynman and Kac are employed to calculate the FPT and the average work for this process. From these results, we obtain an explicit form of the time-cost trade-off relation, which provides the lower bound of the mean FPT for a given work input when the trapping potential is linear. This trade-off relation clearly shows that instantaneous resetting is achievable only when an infinite amount of work is provided. More surprisingly, the trade-off relation derived from the linear potential seems to be valid for a wide range of trapping potentials. In addition, we have also shown that the fixed-time or sharp resetting can further enhance the trade-off relation compared to that of the stochastic resetting.

DOI: [10.1103/PhysRevE.108.044117](https://doi.org/10.1103/PhysRevE.108.044117)**I. INTRODUCTION**

Reset refers to a process that completely erases information pertaining to the current state of a system and returns the system to a predetermined setting. Due to the irreversible nature of the erasure process, a certain thermodynamic cost is required for physical implementation of the reset. According to Landauer's principle, the minimum cost for information erasure is $k_B T \ln 2$ of dissipated heat to reset one bit of information [1,2], where k_B is the Boltzmann constant and T is the environmental temperature. This minimum bound is attainable only in a quasistatic process, which takes an infinitely long time. To reduce the reset time, additional cost should be incurred [3–9]. This indicates the existence of a time-cost trade-off for the reset process, implying that less energy consumption requires more time and vice versa; this trade-off fundamentally constrains the performance of the reset process [10,11]. It will be demonstrated that the trade-off relation prevents instantaneous reset (zero reset time) unless an infinite amount of energy is provided, which is not feasible in the real world. Consequently, study on the minimal time of a process accompanied with resetting should take into account the thermodynamic trade-off relations which have been a prominent topic in the field of stochastic thermodynamics for the past decade [12–22].

Interestingly, it has recently been verified that resetting is an important mechanism to boost the speed of target searching using a random walker [23–36]. This target-searching strategy, referred to as *stochastic resetting*, is crucial for speeding up several biological processes such as kinetic proofreading [37,38], the chaperone-assisted protein-folding

process [39–41], molecular transport [42], and chemical reaction [43]. For example, protein-folding dynamics can be viewed as a random walk construct, which starts from an initial unfolded state and then searches for the target (native state) in a rugged free-energy landscape, as shown in Fig. 1(a). During the process, proteins are sometimes trapped in a local minima (misfolded state), which significantly prolongs the search time. The chaperone assists in restoring misfolded proteins back to the initial unfolded state. Then, the search begins again. This reset significantly reduces the target-searching time. However, the ATP hydrolysis is necessary for chaperone-assisted resetting of the misfolded protein. This example clearly shows that the time for searching, accompanied by stochastic resetting, should be limited by the thermodynamic cost.

Previous studies on stochastic resetting focused mostly on the search time when the resetting occurs instantaneously with limited interests to the understanding of stochastic thermodynamics for such processes [44–46]. This leads us to believe that perhaps a more proper question regarding stochastic resetting in reality would be “What is the minimum search time for a given limited energetic cost?,” which is the main subject of this study. To answer this, we go beyond the instantaneous resetting and consider a realistic *finite-time* reset process that is implemented by a trapping potential [47–54]. For such a setup, we evaluate the total work for reset and the global first passage time (FPT), which includes the time for reset. Based on these results, we derive a time-cost trade-off relation for stochastic resetting with finite time returns. Although this trade-off relation is derived only for a linear potential case, we numerically demonstrate its validity for a wide range of

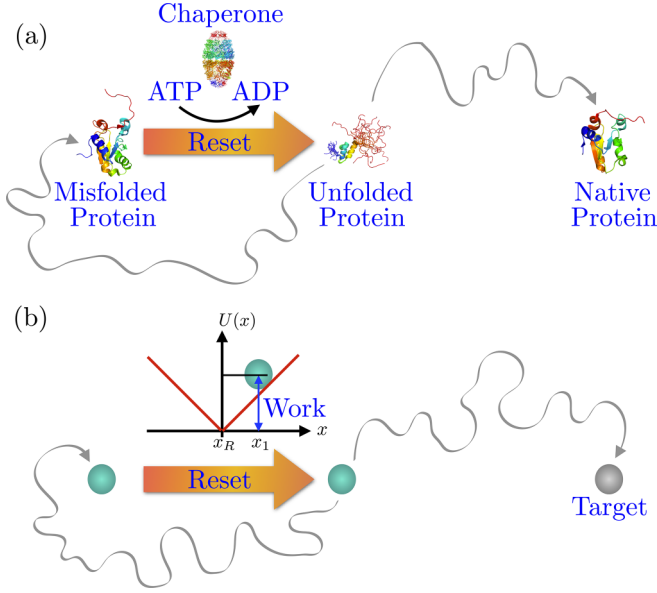


FIG. 1. Schematics of finite-time stochastic resetting processes. (a) Chaperone-assisted protein folding dynamics, from an initial unfolded state to a final native state, in a rugged free-energy landscape. When the protein is trapped in a local minima (misfolded state), a chaperone assists the protein to be reset to the initial unfolded state. (b) Stochastic resetting run by a Brownian particle. At a random time with a fixed rate, the position of the particle is reset by applying an external potential centered around the reset position.

trapping potentials. In addition, we show that the trade-off relation can be further enhanced when the resets occur after fixed time intervals, and not at random time intervals.

II. SETUP

We consider a stochastic resetting process for a one-dimensional Brownian particle in an overdamped environment, as shown in Fig. 1(b). The particle undergoes free-diffusion motion (with diffusion constant D) in the diffusion phase starting from an initial position x_0 . At a random time drawn from an exponential distribution $f_R(t) = re^{-rt}$, where r is the rate, a potential $U(x)$ is turned ON in order to bring the particle to a predetermined reset position x_R . The potential is maintained ON until the particle reaches x_R with a different diffusion constant D_R (the reset or return phase). As soon as the particle reaches x_R , the potential is turned OFF and the particle resumes its free diffusion motion. This diffusion and resetting process is repeated until the particle reaches or finds the target position at x_T during its diffusive phase [55]. We set x_T to the origin without loss of generality. This process corresponds to the A process in Fig. 2 and can be described by the following Langevin equations:

$$\dot{x} = \begin{cases} \sqrt{2D}\eta(t), & \text{diffusion phase,} \\ -\partial_x U(x) + \sqrt{2D_R}\eta(t), & \text{reset phase,} \end{cases} \quad (1)$$

where $\eta(t)$ is a Gaussian white noise with zero mean and unit variance. The global FPT t_G is given by $t_G = t_D + t_R$ (see the A process in Fig. 2), where t_D and t_R are the time spent in the diffusion and reset phases until the particle reaches the

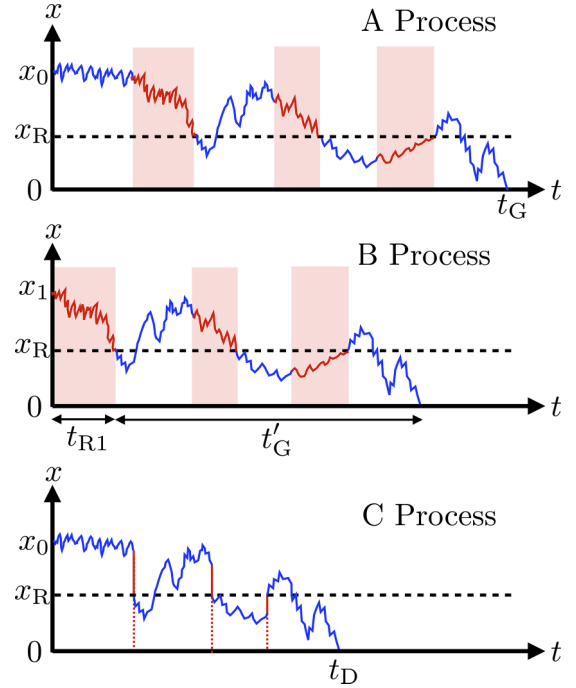


FIG. 2. Stochastic resetting trajectories of A, B, and C processes. The A process starts from x_0 in the diffusion phase, and then, sequential reset (red-shaded region) and diffusion (unshaded region) phases continue until the particle touches the target. The FPT for the A process is given by $t_G = t_D + t_R$. The B process starts from x_1 in the reset phase with the duration t_{R1} , and then, sequential diffusion and reset phases continue until the particle touches the target with the duration t'_G . The C process is obtained by eliminating all the reset phases of the A process, and thus the FPT of the C process is simply given by t_D .

target, respectively. We note that t_D corresponds to the FPT when the reset is instantaneous (see the C process in Fig. 2). Such a stochastic resetting process with stochastic returns using an external trap was introduced in Refs. [53,54] where various nonequilibrium properties such as the steady-state and relaxation phenomena were studied. Evidently, our model (1) is a generalization of those in Refs. [50,52], where only the deterministic dynamics of the reset phase, i.e., $D_R = 0$, was considered.

III. FIRST PASSAGE TIME

Inspired by the Brownian functional method [56,57], we introduce the iterative generating function method to evaluate the n th moment of t_G . First, the moment generating function of t_G for the A process (starting in the diffusion phase) can be written as

$$\mathcal{Q}_A(p|x_0) = \int_0^\infty dt_G e^{-pt_G} P_A(t_G|x_0) \equiv \langle e^{-pt_G} \rangle, \quad (2)$$

where $P_A(t_G|x)$ is the probability density function of t_G for the A process with the initial position x .

Now we consider the B process as illustrated in Fig. 2 for subsequent utilization in the calculation of Eq. (6); it starts from x_1 in the reset phase and terminates when the particle touches the target (origin) in the diffusion phase. The B

process can be divided into two parts; the first reset phase and the remaining part with durations t_{R1} and t'_G , respectively. Then, the moment generating function of the global FPT for the B process, $t_{R1} + t'_G$, can be written as

$$Q_B(p|x_1) = \int_0^\infty dt_{R1} \int_0^\infty dt'_G e^{-p(t_{R1}+t'_G)} P_B(t_{R1}, t'_G|x_1), \quad (3)$$

where $P_B(t_{R1}, t'_G|x_1)$ is the joint probability density function of t_{R1} and t'_G for the B process with the initial position x_1 . As t_{R1} and t'_G are independent variables, $P_B(t_{R1}, t'_G|x_1) = P_R(t_{R1}|x_1)P_A(t'_G|x_R)$, where $P_R(t|x)$ is the probability density function for a single reset phase taking time t with the initial position x . Consequently, $Q_B(p|x_1)$ can be expressed in a product form as

$$Q_B(p|x_1) = Q_R(p|x_1)Q_A(p|x_R), \quad (4)$$

where $Q_R(p|x_1)$ is the momentum generating function of the FPT for a single reset phase defined as

$$Q_R(p|x) = \int_0^\infty dt e^{-pt} P_R(t|x). \quad (5)$$

See Appendix A for detailed calculation of $Q_R(p|x)$.

Now we construct a differential equation for $Q_A(p|x_0)$ with respect to x_0 . We divide the A process with the duration t_G into the initial infinitesimal part with the duration Δt and the remaining part with the duration $t_G - \Delta t$. During the first infinitesimal diffusion process, the dynamics may be switched into the reset phase with the probability $r\Delta t$ (reset rate r), and then the remaining process becomes the B process starting from $x'_0 \equiv x(\Delta t) = x_0 + \sqrt{2D}\eta(0)\Delta t$. Otherwise, the diffusion phase continues with the probability $1 - r\Delta t$ and then the remaining one becomes the A process starting from x'_0 . Therefore, one can write $Q_A(p|x_0)$ in an iterative way as

$$\begin{aligned} Q_A(p|x_0) &= e^{-p\Delta t} \langle e^{-p(t_G - \Delta t)} \rangle \\ &= e^{-p\Delta t} \langle Q_A(p|x'_0)(1 - r\Delta t) + Q_B(p|x'_0)r\Delta t \rangle. \end{aligned} \quad (6)$$

Equation (6) is iterative in $Q_A(p|x)$, since $Q_B(p|x'_0)$ can be replaced by $Q_A(p|x)$ from Eq. (4). By expanding Eq. (6) and keeping terms up to the order of Δt , one can obtain the following backward differential equation of $Q_A(p|x_0)$:

$$[D\partial_{x_0}^2 - (p+r)]Q_A(p|x_0) + rQ_R(p|x_0)Q_A(p|x_R) = 0. \quad (7)$$

By solving Eq. (7), one can obtain $Q_A(p|x_0)$. Then, the m th moment of t_G can be calculated as

$$\langle t_G^m \rangle = (-1)^m \partial_p^m Q_A(p|x_0)|_{p \rightarrow 0}. \quad (8)$$

IV. WORK FOR RESET

Work fluctuations in resetting processes have been of topical interest in recent times (see Refs. [58,59]). However, all these works measure work due to the modulation of an external control parameter. In contrast, in our setup, work is done when the external potential is switched on at the beginning of every reset phase and thus the Brownian particle gains energy from the external potential. Since the potential has no time dependence during the reset phase, there is no further work done on the particle. Note that the potential energy gained by the particle is completely dissipated as heat throughout the

reset phase. Suppose there is a single stochastic trajectory, as shown in the A process of Fig. 2, where each reset phase starts at time t_i ($i = 1, 2, \dots$). The total work W for the trajectory is calculated as the sum of the potential values evaluated at t_i , with the potential set to zero at the reset point. This summation can be expressed more generally by the *counting functional*:

$$V[x(t)] = \int_0^{t_G} Z[x(t)]dt, \quad (9)$$

where $Z[x(t)] = \sum_i \delta(t - t_i)w[x(t)]$ with a weight function $w[x(t)]$ evaluated at t . This functional yields the quantities related to the number of resets during the whole process: For instance, when $w(x) = 1$, $V[x(t)]$ yields the total number of resets during the process, and when $w(x) = U(x)$, $V[x(t)]$ corresponds to the total work W .

Evaluating the general moments of V can be conveniently carried out by considering the trajectory of the C process as shown in Fig. 2, which is obtained by eliminating all reset phases from the original trajectory of the A process. It is important to note that the counting functional V yields the same value for both trajectories. In fact, the trajectory of the C process corresponds to that of *instantaneous* resetting. Thus, Eq. (9) can be evaluated on the corresponding trajectory of the C process with $V[x(t)] = \int_0^{t_G} Z[x(t)]dt$. The generating function for V is then given as

$$Q_C(p|x_0) = \int_0^\infty dV e^{-pV} P_C(V|x_0) \equiv \langle e^{-pV} \rangle, \quad (10)$$

where $P_C(V|x_0)$ is the probability density function of V for the C process. By dividing $V[x(t)]$ into the initial infinitesimal part with the duration Δt and the remaining part as $V[x(t)] = Z[x(0)]\Delta t + \int_{\Delta t}^{t_G} Z[x(t)]dt$, one can rewrite Eq. (10) as

$$Q_C(p|x_0) = \langle e^{-pZ[x(0)]\Delta t} e^{-p \int_{\Delta t}^{t_G} Z[x(t)]dt} \rangle. \quad (11)$$

During the initial infinitesimal process, resetting occurs with the probability $r\Delta t$. Then the next position x'_0 is reset to x_R and $Z[x(0)]\Delta t = w(x_0)$. Otherwise, with the probability $1 - r\Delta t$, the diffusion phase continues, and thus, $x'_0 = x_0 + \sqrt{2D}\eta(0)\Delta t$ and $Z[x(0)]\Delta t = 0$. Similar to Eq. (6), Eq. (11) can be written as

$$\begin{aligned} Q_C(p|x_0) &= (1 - r\Delta t) \langle Q_C(p|x_0 + \sqrt{2D}\eta(0)\Delta t) \rangle \\ &\quad + r\Delta t e^{-pw(x_0)} Q_C(p|x_R). \end{aligned} \quad (12)$$

By keeping terms up to the order of Δt , we finally arrive at the following backward differential equation of $Q_C(p|x_0)$:

$$[D\partial_{x_0}^2 - r]Q_C(p|x_0) + re^{-pw(x_0)} Q_C(p|x_R) = 0. \quad (13)$$

The m th moment of V is then calculated as

$$\langle V^m \rangle = (-1)^m \partial_p^m Q_C(p|x_0)|_{p \rightarrow 0}. \quad (14)$$

V. LINEAR POTENTIAL CASE

We analytically solve the backward differential equations, Eqs. (7) and (13), for a linear potential in x as

$$U(x) = a|x - x_R|^n, \quad (15)$$

with $a > 0$ and $n = 1$. This linear potential leads to $Q_R(p|x) = e^{-\lambda(p)|x - x_R|}$, with $\lambda(p) = (\sqrt{a^2 + 4pD_R} -$

$a)/2D_R$. This $Q_R(p|x)$ can be used to solve Eq. (7) explicitly (see Appendix B). In particular, for $x_0 = x_R$, the solution of Eq. (7) is rather simpler as

$$Q_A(p|x_R) = \frac{e^{-\mu(p)x_R}}{f_A(p, x_R)}, \quad (16)$$

where $\mu(p) = \sqrt{(p+r)/D}$ and $f_A(p, x_R) = 1 + \nu(p) - \nu(p)e^{-[\lambda(p)+\mu(p)]x_R} - \frac{2\nu(p)\lambda(p)}{\mu(p)} \sinh[\mu(p)x_R]e^{-\mu(p)x_R}$, with $\nu(p) = r/[D\lambda^2(p) - (p+r)]$. The mean FPT is then evaluated by utilizing Eq. (8). The result is

$$\begin{aligned} \langle t_G \rangle &= -\partial_p Q_A(p|x_R)|_{p \rightarrow 0} \\ &= \langle t_D \rangle + \frac{1}{\alpha} [2 \sinh(\alpha x_R) - \alpha x_R], \end{aligned} \quad (17)$$

where $\alpha = \sqrt{r/D}$ and $\langle t_D \rangle = (e^{\alpha x_R} - 1)/r$ is the mean FPT with the instantaneous resetting strategy [23]. The detailed derivations for Eqs. (16) and (17) are provided in Appendix B. The second term of the right-hand side in Eq. (17) represents the (positive) extra time due to our finite-time reset strategy. As $a \rightarrow \infty$ (infinitely steep potential), this extra time vanishes, thus representing the limit of instantaneous resetting.

To evaluate the total work, we substitute $w[x(t)] = a|x - x_R|$ into Eq. (13) and solve for $Q_C(p|x_0)$, with $x_0 = x_R$. We find

$$Q_C(p|x_R) = \frac{e^{-\alpha x_R}}{f_C(p, x_R)}, \quad (18)$$

where $f_C(p, x_R) = 1 + \gamma(p) - \gamma(p)e^{-(pa+\alpha)x_R} - \frac{2pa}{\alpha} \gamma(p) \sinh(\alpha x_R) e^{-\alpha x_R}$, with $\gamma(p) = r/(Da^2 p^2 - r)$. The mean total work is then calculated as

$$\begin{aligned} \langle W \rangle &= -\partial_p Q_C(p|x_R)|_{p \rightarrow 0} \\ &= \frac{a}{\alpha} [2 \sinh(\alpha x_R) - \alpha x_R]. \end{aligned} \quad (19)$$

Note that the work diverges in the $a \rightarrow \infty$ limit (instantaneous resetting), indicating an intrinsic trade-off between time and cost. The detailed derivation for Eqs. (18) and (19) are provided in Appendix C. We now turn our attention to another interesting limit $r \rightarrow 0$ (thus, $\alpha \rightarrow 0$). Intuitively, one would expect the average work to be zero in this limit since no work is done without resetting. However, following Eq. (19), one finds $\lim_{r \rightarrow 0} \langle W \rangle = \alpha x_R$, which is a finite nonzero quantity that depends on the potential strength. This implies that the limit of the zero resetting rate is not equivalent to the bare process where no reset takes place at all. Thus, there exists a discontinuity in the average work at $r = 0$. This is attributed to the fact that the average number of resets vanishes as αx_R , but the work per one reset diverges as a/α , since the particle diffuses far away from the origin for a long duration before reset occurs. For this reason, mean work remains to be finite in the limit $r \rightarrow 0$.

Figure 3(a) displays the plot for $\langle t_G \rangle$ versus r for various values of a , which indicates that simulation results agree well with Eq. (17). Note that $D = 0.5$ is used for all numerical calculations throughout this study. As shown in the figure, $\langle t_G \rangle$ is a nonmonotonic function of r ; thus, it is minimized at some optimal rate $r = r_G^*$ which is the solution of $\partial_r \langle t_G \rangle = 0$. As expected, $\langle t_G \rangle$ approaches $\langle t_D \rangle$ as a increases. It has been demonstrated in the figure at the end of Appendix B,

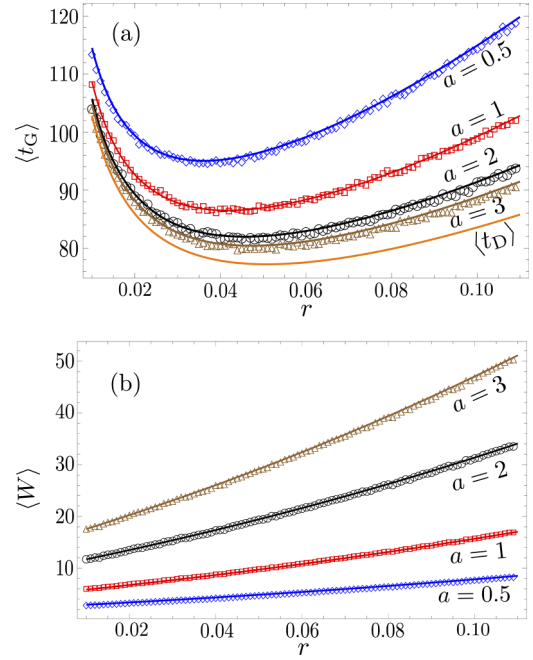


FIG. 3. Analytic and numerical results for stochastic resetting with finite-time reset. Plots for (a) $\langle t_G \rangle$ and (b) $\langle W \rangle$ as a function of r for various values of a with the parameters $x_0 = x_R = 5$ and $D = D_R = 0.5$. The solid curves of plots (a) and (b) represent the analytic results obtained from Eqs. (17) and (19), respectively. All data points are obtained by averaging over 10^5 trajectories.

that r_G^* and $\langle t_G \rangle|_{r=r_G^*}$ saturate the optimal rate r_D^* (solution of $\partial_r \langle t_D \rangle = 0$) and the corresponding mean FPT $\langle t_D \rangle|_{r=r_D^*}$ for instantaneous resetting, respectively. Figure 3(b) displays the plot of $\langle W \rangle$ versus r . In contrast to $\langle t_G \rangle$, $\langle W \rangle$ is a monotonically increasing function of both r and a . Simulation data are in excellent agreement with Eq. (19).

We note that the mean FPT, Eq. (17), is independent of D_R . In fact, Eq. (17) is exactly the expression for the mean FPT as was obtained for the model with $D_R = 0$ in Refs. [50,52]. This is because the return time due to dragging with a constant velocity as was done in Refs. [50,52] is identical to the return time due to stochastic return (only in the mean level). However, the fluctuations in FPT and the role of higher-order potentials should have different results compared to those with the deterministic reset dynamics. This point is emphasized in Fig. 4, which is the plot for the standard deviation of the global FPT $\sigma \equiv \sqrt{\langle t_G^2 \rangle - \langle t_G \rangle^2}$ as a function of r for various D_R . The curves in the plot are evaluated from Eq. (8). This plot clearly demonstrates that the fluctuation of the FPT depends on D_R .

VI. TRADE-OFF RELATION

It is evident that instantaneous resetting is not possible unless an infinite amount of work is provided. Thus, in order to address the physically meaningful question ‘‘What is the minimum FPT for a given cost?,’’ we reformulate the mean FPT $\langle t_G \rangle$ in terms of work $\langle W \rangle$ instead of the potential strength

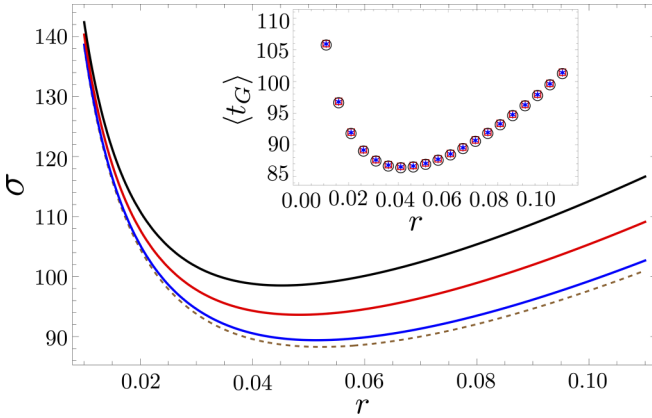


FIG. 4. Standard deviation of the global FPT as a function of the resetting rate r for different values of $D_R = 0$ (brown dashed line), $D_R = 10$ (blue line), 50 (red line), and 100 (black line). (Inset) Mean FPT for different values of D_R which shows its invariance under D_R modulation unlike the standard deviation σ .

a , using Eqs. (17) and (19), as

$$\langle t_G \rangle = \langle t_D \rangle + \frac{1}{\alpha^2 \langle W \rangle} [2 \sinh(\alpha x_R) - \alpha x_R]^2. \quad (20)$$

Equation (20) clearly shows the trade-off relation between the mean FPT and average work: Large work leads to small time, and vice versa. We introduce the notion of *excess* time $\langle t_{\text{ex}} \rangle$ as the mean FPT with reference to the minimal mean FPT for instantaneous resetting, i.e.,

$$\langle t_{\text{ex}} \rangle \equiv \langle t_G \rangle - \langle t_D \rangle|_{r=r_D^*}, \quad (21)$$

where $r = r_D^*$ is the optimal resetting rate at which the mean FPT, with instantaneous resetting strategy, $\langle t_D \rangle$ is minimum. By solving $\partial_r \langle t_{\text{ex}} \rangle = 0$ for fixed $\langle W \rangle$, we determine the resetting rate $r = r_{\text{ex}}^*$ that minimizes $\langle t_{\text{ex}} \rangle$. The minimum excess time $\langle t_{\text{ex}} \rangle|_{r=r_{\text{ex}}^*}$ is plotted (with a black solid line) against $\langle W \rangle$

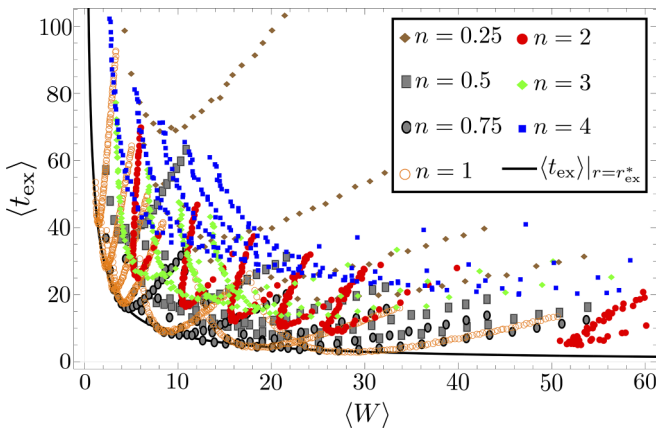


FIG. 5. Trade-off relation between excess time and work, i.e., plot of $\langle t_{\text{ex}} \rangle$ as a function of $\langle W \rangle$. The solid curve denotes the minimum excess time $\langle t_{\text{ex}} \rangle|_{r=r_{\text{ex}}^*}$ for a given work, derived for $n = 1$. Data points are obtained from the simulation with various potential strengths a , reset rates r , and potential exponents n . Each point is obtained by averaging over 10^5 trajectories.

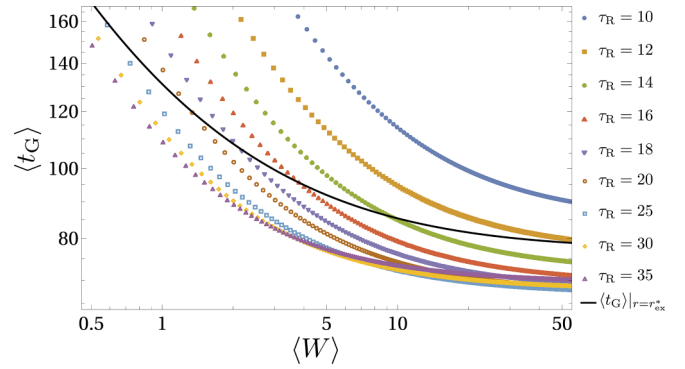


FIG. 6. Trade-off relation between mean FPT and average work. The solid curve denotes the minimum value of the global FPT $\langle t_G \rangle|_{r=r_{\text{ex}}^*}$ for the Poissonian (stochastic) resetting protocol. Data points are obtained by numerical calculation of the mean FPT and $\langle W \rangle$ for the sharp resetting protocol for various τ_R 's.

in Fig. 5, which serves as the lower bound of $\langle t_{\text{ex}} \rangle$ for the $n = 1$ case.

To verify this, we first performed numerical simulations to obtain $\langle t_{\text{ex}} \rangle$ and $\langle W \rangle$ for the $n = 1$ case and constructed a trade-off plot as shown in Fig. 5. Each point there for a given resetting rate and a is denoted by an orange open circle. More data points are obtained by varying a and r in the ranges $0.2 \leq a \leq 3$ and $0.005 \leq r \leq 0.1$. See also Appendix C where we have illustrated the case of $n = 1$ in detail. As shown in the figure, all data points are above the lower bound curve $\langle t_{\text{ex}} \rangle|_{r=r_{\text{ex}}^*}$. We repeated the same simulations for different potentials by varying n , i.e., $n = 0.25, 0.5, 0.75, 2, 3$, and 4, keeping the same variation for a and r . The results are also plotted in Fig. 5. Surprisingly, for any value of n , all the data remain lower bounded by the minimum curve for $n = 1$. This suggests that the minimum curve derived from the linear potential could serve as the lower bound of a universal time-cost trade-off relation for general finite-time stochastic resetting processes. Further study is necessary for elucidating the optimality of the bound.

Since our primary goal is to minimize the mean FPT for given energy resources, it will be worthwhile to investigate other resetting strategies. In Refs. [32,60], it was shown that the sharp resetting strategy—where the resetting is conducted stroboscopically i.e., after every fixed time interval τ_R —can render the mean FPT globally optimized in the case of instantaneous resetting. It is, thus, natural to investigate the trade-off relation when sharp resetting is employed in the case of finite-time return. We have calculated the mean FPT and the average work for a Brownian particle undergoing a finite-time resetting process using a sharp resetting protocol (details provided in Appendix D). In Fig. 6, the FPT for the sharp resetting protocol is plotted against the average work done on the system for different τ_R 's. For comparison purpose, we also draw the optimal bound curve $\langle t_G \rangle|_{r=r_{\text{ex}}^*}$ of the stochastic (Poissonian) resetting protocol, which is essentially the same curve presented in Fig. 5. It is important to note that for some values of τ_R , the trade-off curve for the sharp resetting protocol is well below the curve of $\langle t_G \rangle|_{r=r_{\text{ex}}^*}$. This implies that for fixed energy resources, the mean FPT can be further lowered using a sharp resetting protocol.

VII. CONCLUSION

In this study, we examined the thermodynamic cost and the first-passage time (FPT) of the stochastic resetting process, in which the reset is implemented using the trapping potential given by Eq. (15). We find a time-cost trade-off relation in stochastic resetting, where the minimum FPT can be decreased with increased work, and vice versa. Our result clearly demonstrates that, while instantaneous resetting is always faster in target-searching, it requires an infinite cost, making it neither practical nor efficient from the viewpoint of energetics. The trade-off relation we found appears to be valid for a wide range of trapping potentials. Therefore, this trade-off relation could be used as a standard reference for investigating various processes accompanied with a finite-time stochastic resetting process, where the reset is not controllable but occurs at random times such as in biological systems. However, in the case where the reset is controllable such as in some artificial systems, the trade-off minima curve can be further lowered by using a different resetting strategy, namely, the sharp resetting protocol. Our results could lead to the construction of thermodynamically efficient searching strategies with finite energy resources, which could be especially useful in experimental studies of biophysical and single-particle systems [37–41,61,62] pertaining to finite-time stochastic resetting.

ACKNOWLEDGMENTS

We thank Changbong Hyun for many useful discussions and providing us the figures of proteins. The authors acknowledge the Korea Institute for Advanced Study for providing computing resources (KIAS Center for Advanced Computation Linux Cluster System). This research was supported by NRF Grant No. 2017R1D1A1B06035497 (H.P.) and individual KIAS Grants No. PG064901 (J.S.L.), No. PG085601 (P.S.P), and No. QP013601 (H.P.) at the Korea Institute for Advanced Study. A.P. gratefully acknowledges research support from DST-SERB Start-up Research Grant No. SRG/2022/000080 and the DAE, Government of India.

APPENDIX A: MOMENT GENERATING FUNCTION OF FPT IN A SINGLE RESET PHASE

We consider a Brownian particle moving in an external potential $U(x)$ that is centered around the resetting position x_R . The dynamics of the particle is described by the following Langevin equation

$$\dot{x} = -\partial_x U(x) + \sqrt{2D_R}\eta(t), \quad (\text{A1})$$

where $\eta(t)$ is a Gaussian white noise with zero mean and unit variance, and D_R is the diffusion constant for the reset phase. The particle starts at a position x_1 and we want to find the time when it reaches the position x_R for the first time. This is a typical reset phase scenario in a resetting dynamics with finite reset time.

The moment generating function of the FPT t_R to return to the resetting position can be written as

$$Q_R(p|x_1) = \int_0^\infty e^{-pt_R} P_R(t_R|x_1) dt_R = \langle e^{-pt_R} \rangle, \quad (\text{A2})$$

where $P_R(t_R|x_1)$ is the probability density function of t_R given the particle starts the reset phase from the position x_1 . Now we divide the FPT of the reset process t_R into two parts: The initial infinitesimal time Δt and the remaining time $t_R - \Delta t$. The position at time $t = \Delta t$ is given by $x'_1 = x_1 + [-\partial_x U(x) + \sqrt{2D_R}\eta(t)]\Delta t$. Therefore, the expression of $Q_R(p|x_1)$ can be rewritten as

$$\begin{aligned} Q_R(p|x_1) &= \langle e^{-p\Delta t} Q_R(p|x'_1) \rangle \\ &\approx (1 - p\Delta t) \langle Q_R(p|x_1 - \partial_{x_1} U \Delta t + \sqrt{2D_R}\eta(0)\Delta t) \rangle \\ &\approx (1 - p\Delta t) \langle Q_R(p|x_1) + \partial_{x_1} Q_R(p|x_1) \{-\partial_{x_1} U \\ &\quad + \sqrt{2D_R}\eta(0)\} \Delta t + \frac{1}{2} \partial_{x_1}^2 Q_R(p|x_1) \{-\partial_{x_1} U \\ &\quad + \sqrt{2D_R}\eta(0)\}^2 (\Delta t)^2 \rangle \\ &\approx Q_R(p|x_1) - pQ_R(p|x_1)\Delta t - (\partial_{x_1} U) \partial_{x_1} Q_R(p|x_1)\Delta t \\ &\quad + D_R \partial_{x_1}^2 Q_R(p|x_1)\Delta t. \end{aligned}$$

Hence, the backward differential equation of the moment generating function for the reset phase can be written as

$$D_R \partial_{x_1}^2 Q_R(p|x_1) - (\partial_{x_1} U) \partial_{x_1} Q_R(p|x_1) - pQ_R(p|x_1) = 0. \quad (\text{A3})$$

The boundary conditions for solving the above equation for $p > 0$ are $Q_R(p|x_1 \rightarrow x_R) = 1$ and $Q_R(p|x_1 \rightarrow \pm\infty) = 0$, with $Q_R(0|x_1) = 1$. Since we are interested in the derivative of $Q_R(p|x_1)$ with respect to p at $p = 0$, it is not necessary to consider the case for $p < 0$. We consider a linear trapping potential $U(x) = a|x_1 - x_R|$ ($a > 0$), yielding

$$\begin{aligned} -\partial_{x_1} U &= -a, \quad x_1 \geq x_R, \\ &= a, \quad x_1 < x_R. \end{aligned}$$

In the region $x_1 \geq x_R$, Eq. (A3) is written as

$$D_R \partial_{x_1}^2 Q_R(p|x_1) - a \partial_{x_1} Q_R(p|x_1) - pQ_R(p|x_1) = 0. \quad (\text{A4})$$

The solution of the above equation is given by

$$Q_R(p|x_1) = C_1 e^{\lambda^+ x_1} + C_2 e^{\lambda^- x_1}, \quad (\text{A5})$$

where $\lambda^\pm = \frac{a \pm \sqrt{a^2 + 4pD_R}}{2D_R}$. Using the boundary condition $Q_R(p|x_1 \rightarrow \infty) = 0 \Rightarrow C_1 = 0$ and using $Q_R(p|x_1 \rightarrow x_R) = 1 \Rightarrow C_2 = e^{-\lambda^- x_R}$. Hence, for $x_1 \geq x_R$,

$$Q_R(p|x_1) = \exp \left[-\frac{\sqrt{a^2 + 4pD_R} - a}{2D_R} (x_1 - x_R) \right]. \quad (\text{A6})$$

In the region $x_1 < x_R$, Eq. (A3) is written as

$$D_R \partial_{x_1}^2 Q_R(p|x_1) + a \partial_{x_1} Q_R(p|x_1) - pQ_R(p|x_1) = 0. \quad (\text{A7})$$

The solution of the above equation (A7) is given by

$$Q_R(p|x_1) = C_1 e^{\lambda^+ x_1} + C_2 e^{\lambda^- x_1}, \quad (\text{A8})$$

where $\lambda^\pm = \frac{-a \pm \sqrt{a^2 + 4pD_R}}{2D_R}$. Using the boundary condition $Q_R(p|x_1 \rightarrow -\infty) = 0 \Rightarrow C_2 = 0$ and using $Q_R(p|x_1 \rightarrow x_R) = 1 \Rightarrow C_1 = e^{-\lambda^+ x_R}$. Hence, for $x_1 < x_R$,

$$Q_R(p|x_1) = \exp \left[-\frac{\sqrt{a^2 + 4pD_R} - a}{2D_R} (x_R - x_1) \right]. \quad (\text{A9})$$

Combining the two expressions in Eqs. (A6) and (A9), the moment generating function is

$$Q_R(p|x_1) = \exp\left[-\frac{\sqrt{a^2 + 4pD_R} - a}{2D_R}|x_1 - x_R|\right]. \quad (\text{A10})$$

APPENDIX B: CALCULATION OF THE GLOBAL FPT

The backward differential equation of $Q_A(p|x_0)$ is given by

$$D\partial_{x_0}^2 Q_A(p|x_0) - (p+r)Q_A(p|x_0) + rQ_A(p|x_R)Q_R(p|x_0) = 0. \quad (\text{B1})$$

Using Eq. (A10), the above equation can be rewritten as

$$D\partial_{x_0}^2 Q_A(p|x_0) - (p+r)Q_A(p|x_0) + r \exp[-\lambda(p)|x_0 - x_R|]Q_A(p|x_R) = 0, \quad (\text{B2})$$

where $\lambda(p) = \frac{\sqrt{a^2 + 4pD_R} - a}{2D_R}$. The above equation (B2) is solved in two regions, namely, Region I: $x_0 > x_R$, and Region II: $x_0 < x_R$. In Region I, Eq. (B2) can be written as

$$D\partial_{x_0}^2 Q_A^I(p|x_0) - (p+r)Q_A^I(p|x_0) + r \exp[-\lambda(p)(x_0 - x_R)]Q_A(p|x_R) = 0. \quad (\text{B3})$$

The solution of Eq. (B3) is

$$Q_A^I(p|x_0) = C_1 e^{\mu(p)x_0} + C_2 e^{-\mu(p)x_0} - v(p)Q_A(p|x_R)e^{-\lambda(p)(x_0 - x_R)}, \quad (\text{B4})$$

where $\mu(p) = \sqrt{(p+r)/D}$ and $v(p) = r/[D\lambda^2(p) - (p+r)]$. In Region II, Eq. (B2) can be written as

$$D\partial_{x_0}^2 Q_A^{II}(p|x_0) - (p+r)Q_A^{II}(p|x_0) + r \exp[-\lambda(p)(x_R - x_0)]Q_A(p|x_R) = 0. \quad (\text{B5})$$

The solution of Eq. (B5) is

$$Q_A^{II}(p|x_0) = C_3 e^{\mu(p)x_0} + C_4 e^{-\mu(p)x_0} - v(p)Q_A(p|x_R)e^{-\lambda(p)(x_R - x_0)}. \quad (\text{B6})$$

The constants in the above expressions (B4) and (B6) for $Q_A^I(p|x_0)$ and $Q_A^{II}(p|x_0)$ are determined by the following four boundary conditions: (i) $Q_A^I(p|x_0 \rightarrow \infty) = 0$, (ii) $Q_A^{II}(p|x_0 \rightarrow 0) = 1$, (iii) $Q_A^I(p|x_0 \rightarrow x_R^+) = Q_A^{II}(p|x_0 \rightarrow x_R^-) = Q_A(p|x_R)$, and (iv) $\partial_{x_0} Q_A^I(p|x_0)|_{x_0 \rightarrow x_R^+} = \partial_{x_0} Q_A^{II}(p|x_0)|_{x_0 \rightarrow x_R^-}$.

Boundary condition (i) suggests $C_1 = 0$. Using boundary condition (ii), we have

$$C_3 + C_4 - v(p)e^{-\lambda(p)x_R}Q_A(p|x_R) = 1. \quad (\text{B7})$$

Using boundary condition (iii), we get

$$C_2 e^{-\mu(p)x_R} - v(p)Q_A(p|x_R) = C_3 e^{\mu(p)x_R} + C_4 e^{-\mu(p)x_R} - v(p)Q_A(p|x_R) \Rightarrow C_2 = C_3 e^{2\mu(p)x_R} + C_4. \quad (\text{B8})$$

Using Boundary condition (iv), we have

$$\begin{aligned} -\mu(p)C_2 e^{-\mu(p)x_R} + v(p)\lambda(p)Q_A(p|x_R) &= \mu(p)C_3 e^{\mu(p)x_0} - \mu(p)C_4 e^{-\mu(p)x_0} - v(p)\lambda(p)Q_A(p|x_R), \\ C_2 e^{-\mu(p)x_R} + C_3 e^{\mu(p)x_0} - C_4 e^{-\mu(p)x_0} &= \frac{2v(p)\lambda(p)}{\mu(p)}Q_A(p|x_R), \\ [C_3 e^{2\mu(p)x_R} + C_4]e^{-\mu(p)x_R} + C_3 e^{\mu(p)x_0} - C_4 e^{-\mu(p)x_0} &= \frac{2v(p)\lambda(p)}{\mu(p)}Q_A(p|x_R), \\ 2C_3 e^{\mu(p)x_R} &= \frac{2v(p)\lambda(p)}{\mu(p)}Q_A(p|x_R), \\ \Rightarrow C_3 &= \frac{v(p)\lambda(p)}{\mu(p)}Q_A(p|x_R)e^{-\mu(p)x_R}. \end{aligned} \quad (\text{B9})$$

The expression of C_4 can be calculated by plugging Eq. (B9) into Eq. (B7),

$$C_4 = 1 + v(p)e^{-\lambda(p)x_R}Q_A(p|x_R) - \frac{v(p)\lambda(p)}{\mu(p)}Q_A(p|x_R)e^{-\mu(p)x_R}. \quad (\text{B10})$$

Using the expressions of C_3 and C_4 in Eq. (B8), we have

$$\begin{aligned} C_2 &= \left[\frac{v(p)\lambda(p)}{\mu(p)}Q_A(p|x_R)e^{-\mu(p)x_R} \right] e^{2\mu(p)x_R} + 1 + v(p)e^{-\lambda(p)x_R}Q_A(p|x_R) - \frac{v(p)\lambda(p)}{\mu(p)}Q_A(p|x_R)e^{-\mu(p)x_R} \\ &= 1 + v(p)e^{-\lambda(p)x_R}Q_A(p|x_R) + \frac{v(p)\lambda(p)}{\mu(p)}Q_A(p|x_R)[e^{\mu(p)x_R} - e^{-\mu(p)x_R}] \\ &= 1 + v(p)e^{-\lambda(p)x_R}Q_A(p|x_R) + \frac{2v(p)\lambda(p)}{\mu(p)}Q_A(p|x_R)\sinh[\mu(p)x_R]. \end{aligned} \quad (\text{B11})$$

Hence the expression of the moment generating function in Region I is

$$Q_A^I(p|x_0) = e^{-\mu(p)x_0} + v(p)e^{-\lambda(p)x_R} e^{-\mu(p)x_0} Q_A(p|x_R) + \frac{2v(p)\lambda(p)}{\mu(p)} Q_A(p|x_R) \sinh[\mu(p)x_R] e^{-\mu(p)x_0} - v(p) Q_A(p|x_R) e^{-\lambda(p)(x_0-x_R)}. \tag{B12}$$

The expression of $Q_A(p|x_R)$ can be calculated by replacing x_0 with x_R in Eq. (B12) as

$$Q_A(p|x_R) = e^{-\mu(p)x_R} + \left[v(p)e^{-[\lambda(p)+\mu(p)]x_R} + \frac{2v(p)\lambda(p)}{\mu(p)} \sinh[\mu(p)x_R] e^{-\mu(p)x_R} - v(p) \right] Q_A(p|x_R) \Rightarrow Q_A(p|x_R) = \frac{e^{-\mu(p)x_R}}{1 + v(p) - v(p)e^{-[\lambda(p)+\mu(p)]x_R} - \frac{2v(p)\lambda(p)}{\mu(p)} \sinh[\mu(p)x_R] e^{-\mu(p)x_R}} = \frac{e^{-\mu(p)x_R}}{f_A(p, x_R)}. \tag{B13}$$

Considering the Brownian particle to be reset to its initial position, i.e., $x_0 = x_R$, the FPT to reach the global target at the origin is

$$\begin{aligned} \langle t_G \rangle &= -\partial_p Q_A(p|x_R)|_{p \rightarrow 0} = - \left[-x_R \frac{e^{-\mu(p)x_R}}{f_A(p, x_R)} \partial_p \mu(p) - \frac{e^{-\mu(p)x_R}}{f^2(p|x_R)} \partial_p f_A(p, x_R) \right] \Big|_{p \rightarrow 0} \\ &= [x_R Q_A(p|x_R) \partial_p \mu(p) + e^{\mu(p)x_R} Q_A^2(p|x_R) \partial_p f_A(p, x_R)] \Big|_{p \rightarrow 0} \\ &= x_R Q_A(0|x_R) \partial_p \mu(p)|_{p \rightarrow 0} + e^{\mu(0)x_R} Q_A^2(0|x_R) \partial_p f_A(p, x_R)|_{p \rightarrow 0}. \end{aligned} \tag{B14}$$

In addition, we have

$$\begin{aligned} \mu(p) &= \sqrt{(p+r)/D}; \quad \mu(0) = \sqrt{r/D} = \alpha; \quad \partial_p \mu(p) = \frac{1}{\sqrt{D} 2\sqrt{p+r}}; \quad \partial_p \mu(p)|_{p \rightarrow 0} = \frac{1}{2\sqrt{rD}} = \frac{1}{2D\alpha}, \\ \lambda(p) &= \frac{\sqrt{a^2 + 4pD_R} - a}{2D_R}; \quad \lambda(0) = 0; \quad \partial_p \lambda(p) = \frac{1}{\sqrt{a^2 + 4pD_R}}; \quad \partial_p \lambda(p)|_{p \rightarrow 0} = \frac{1}{a}, \\ v(p) &= \frac{r}{D\lambda^2(p) - (p+r)}; \quad v(0) = \frac{r}{D\lambda^2(0) - r} = -1; \quad \partial_p v(p) = -\frac{r[2D\lambda(p)\partial_p \lambda(p) - 1]}{[D\lambda^2(p) - (p+r)]^2}; \\ \partial_p v(p)|_{p \rightarrow 0} &= -\frac{r[2D\lambda(0)\partial_p \lambda(p)|_{p \rightarrow 0} - 1]}{[D\lambda^2(0) - r]^2} = \frac{1}{r}. \end{aligned} \tag{B15}$$

The above expressions yield

$$\begin{aligned} \partial_p f_A(p, x_R)|_{p \rightarrow 0} &= \partial_p v(p)|_{p \rightarrow 0} - \partial_p v(p)|_{p \rightarrow 0} e^{-[\lambda(0)+\mu(0)]x_R} - v(0)x_R e^{-[\lambda(0)+\mu(0)]x_R} [\partial_p \lambda(p)|_{p \rightarrow 0} + \partial_p \mu(p)|_{p \rightarrow 0}] \\ &\quad - \frac{2v(0)}{\mu(0)} \sinh[\mu(0)x_R] e^{-\mu(0)x_R} \partial_p \lambda(p)|_{p \rightarrow 0} \\ &= \frac{1}{r} - \frac{1}{r} e^{-\alpha x_R} + (-1)x_R e^{-\alpha x_R} \left[\frac{1}{a} + \frac{1}{2\sqrt{rD}} \right] - \frac{2(-1)}{\alpha} \sinh[\alpha x_R] e^{-\alpha x_R} \frac{1}{a} \\ &= \frac{1}{r} (1 - e^{-\alpha x_R}) - x_R e^{-\alpha x_R} \left[\frac{1}{a} + \frac{1}{2D\alpha} \right] + \frac{2}{\alpha a} \sinh[\alpha x_R] e^{-\alpha x_R}, \\ Q_A(0|x_R) &= \frac{e^{-\mu(0)x_R}}{f(0, x_R)} = \frac{e^{-\alpha x_R}}{1 + v(0) - v(0)e^{-[\lambda(0)+\mu(0)]x_R} - \frac{2v(0)\lambda(0)}{\mu(0)} \sinh[\mu(0)x_R] e^{-\mu(0)x_R}} \\ &= \frac{e^{-\alpha x_R}}{1 + (-1) - (-1)e^{-\alpha x_R}} = 1. \end{aligned} \tag{B16}$$

Therefore, the expression of the global mean FPT is

$$\begin{aligned} \langle t_G \rangle &= \frac{x_R}{2D\alpha} + e^{\alpha x_R} \left[\frac{1}{r} (1 - e^{-\alpha x_R}) - x_R e^{-\alpha x_R} \left(\frac{1}{a} + \frac{1}{2D\alpha} \right) + \frac{2}{\alpha a} \sinh(\alpha x_R) e^{-\alpha x_R} \right] \\ &= \frac{x_R}{2D\alpha} + \frac{1}{r} (e^{\alpha x_R} - 1) - \frac{x_R}{a} - \frac{x_R}{2D\alpha} + \frac{1}{\alpha a} \sinh(\alpha x_R) \\ &= \langle t_D \rangle + \frac{1}{\alpha a} [2 \sinh(\alpha x_R) - \alpha x_R], \end{aligned} \tag{B17}$$

where $\langle t_D \rangle = (e^{\alpha x_R} - 1)/r$ is the mean FPT to reach the global target at the origin with instantaneous resetting.

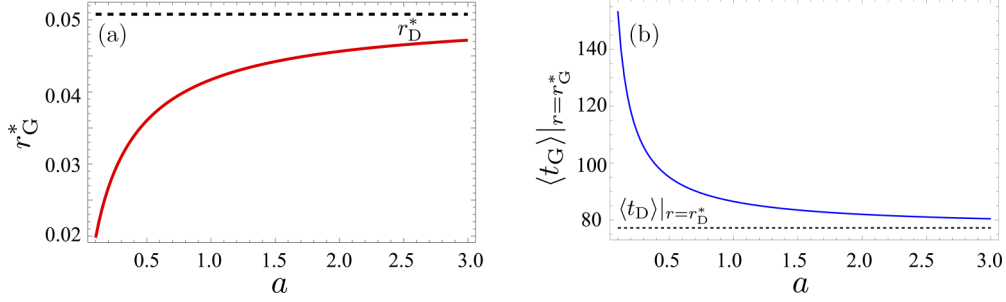


FIG. 7. Analytical plots for linear trapping potential showing the convergence of the results of finite-time stochastic resetting to those of the instantaneous resetting process at large values of strength of the potential a . (a) Plot of the optimal resetting rate r_G^* as a function of the potential strength. (b) Plot of the mean FPT at the optimal resetting rate $r = r_G^*$ as a function of the potential strength. In both plots the black dashed line represents the results of the instantaneous resetting.

The global mean FPT has a minima with respect to the resetting rate (see Fig. 3). The optimal resetting rate and the corresponding minimum mean FPT is plotted against the potential strength in Fig. 7 along with their limiting values.

APPENDIX C: CALCULATION OF WORK

The backward differential equation of $Q_C(p|x_0)$ is given by

$$D\partial_{x_0}^2 Q_C(p|x_0) - rQ_C(p|x_0) + re^{-pw(x_0)} Q_C(p|x_R) = 0. \quad (\text{C1})$$

To calculate work during the whole process, we replace the weight function $w[x(t)]$ with the trapping potential $U(x)$. Hence, for the linear potential, $w[x(t)] = U(x) = a|x - x_R|$ with $a > 0$. In this case Eq. (C1) becomes

$$D\partial_{x_0}^2 Q_C(p|x_0) - rQ_C(p|x_0) + re^{-pa|x_0 - x_R|} Q_C(p|x_R) = 0. \quad (\text{C2})$$

Equation (C2) is solved in two regions, namely, Region I: $x_0 > x_R$, and Region II: $x_0 < x_R$. In Region I, Eq. (C2) can be written as

$$D\partial_{x_0}^2 Q_C^I(p|x_0) - rQ_C^I(p|x_0) + re^{-pa(x_0 - x_R)} Q_C(p|x_R) = 0. \quad (\text{C3})$$

The solution of Eq. (C3) is

$$Q_C^I(p|x_0) = C_1 e^{\alpha x_0} + C_2 e^{-\alpha x_0} - \gamma(p) e^{-pa(x_0 - x_R)} Q_C(p|x_R), \quad (\text{C4})$$

where $\gamma(p) = r/(Dp^2 a^2 - 2r)$. In Region II, Eq. (C2) can be rewritten as

$$D\partial_{x_0}^2 Q_C^{II}(p|x_0) - rQ_C^{II}(p|x_0) + re^{-pa(x_R - x_0)} Q_C(p|x_R) = 0. \quad (\text{C5})$$

The solution of the above equation (C5) is

$$Q_C^{II}(p|x_0) = C_3 e^{\alpha x_0} + C_4 e^{-\alpha x_0} - \gamma(p) e^{-pa(x_R - x_0)} Q_C(p|x_R). \quad (\text{C6})$$

Boundary conditions are as follows: (i) $Q_C^I(p|x_0 \rightarrow \infty) = 0$, (ii) $Q_C^{II}(p|x_0 \rightarrow 0) = 1$, (iii) $Q_C^I(p|x_0 \rightarrow x_R^+) = Q_C^{II}(p|x_0 \rightarrow x_R^-) = Q_C(p|x_R)$, and (iv) $\partial_{x_0} Q_C^I(p|x_0)|_{x_0 \rightarrow x_R^+} = \partial_{x_0} Q_C^{II}(p|x_0)|_{x_0 \rightarrow x_R^-}$.

Boundary condition (i) suggests $C_1 = 0$. Using boundary condition (ii), we have

$$C_3 + C_4 = 1 + \gamma(p) e^{-pa x_R} Q_C(p|x_R). \quad (\text{C7})$$

Using boundary condition (iii), we get

$$\begin{aligned} C_2 e^{-\alpha x_R} - \gamma(p) Q_C(p|x_R) &= C_3 e^{\alpha x_R} + C_4 e^{-\alpha x_R} - \gamma(p) Q_C(p|x_R) \\ \Rightarrow C_2 &= C_3 e^{2\alpha x_R} + C_4. \end{aligned} \quad (\text{C8})$$

Using boundary condition (iv), we obtain

$$\begin{aligned} -\alpha C_2 e^{-\alpha x_R} + pa\gamma(p) Q_C(p|x_R) &= \alpha C_3 e^{\alpha x_R} - \alpha C_4 e^{-\alpha x_R} - pa\gamma(p) Q_C(p|x_R), \\ \alpha[C_2 e^{-\alpha x_R} + C_3 e^{\alpha x_R} - C_4 e^{-\alpha x_R}] &= 2pa\gamma(p) Q_C(p|x_R), \\ C_3 e^{\alpha x_R} + C_4 e^{-\alpha x_R} + C_3 e^{\alpha x_R} - C_4 e^{-\alpha x_R} &= \frac{2pa}{\alpha} \gamma(p) Q_C(p|x_R) \\ \Rightarrow C_3 &= \frac{pa}{\alpha} \gamma(p) Q_C(p|x_R) e^{-\alpha x_R}. \end{aligned} \quad (\text{C9})$$

Using the expression in Eq. (C8), and substituting x_0 with x_R in the expression of $Q^I(p|x_0)$, one arrives at the following expression of $Q_C(p|x_R)$:

$$Q_C(p|x_R) = \frac{e^{-\alpha x_R}}{1 + \gamma(p) - \gamma(p) e^{-(pa + \alpha)x_R} - \frac{2pa}{\alpha} \gamma(p) \sinh(\alpha x_R) e^{-\alpha x_R}} = \frac{e^{-\alpha x_R}}{f_C(p, x_R)}. \quad (\text{C10})$$

Considering the Brownian particle to be reset to its initial position, the average work done until the Brownian particle reaches the target for the first time is

$$\begin{aligned}\langle W \rangle &= -\partial_p Q_C(p|x_R)|_{p \rightarrow 0} = \frac{e^{-\alpha x_R}}{f_C^2(p, x_R)} \partial_p f_C(p, x_R)|_{p \rightarrow 0} \\ &= e^{\alpha x_R} Q_C^2(0|x_R) \partial_p f_C(p, x_R)|_{p \rightarrow 0}.\end{aligned}\quad (\text{C11})$$

Now, we have

$$\begin{aligned}f_C(p, x_R) &= 1 + \gamma(p) - \gamma(p)e^{-(pa+\alpha)x_R} - \frac{2pa}{\alpha} \gamma(p) \sinh(\alpha x_R) e^{-\alpha x_R}, \\ \partial_p f_C(p, x_R) &= \partial_p \gamma(p) - \partial_p \gamma(p) e^{-(pa+\alpha)x_R} + \alpha x_R \gamma(p) e^{-(pa+\alpha)x_R} - \frac{2a}{\alpha} \gamma(p) \sinh(\alpha x_R) e^{-\alpha x_R} \\ &\quad - \frac{2pa}{\alpha} \partial_p \gamma(p) \sinh(\alpha x_R) e^{-\alpha x_R}, \\ \partial_p f_C(p, x_R)|_{p \rightarrow 0} &= \partial_p \gamma(p)|_{p \rightarrow 0} - \partial_p \gamma(p)|_{p \rightarrow 0} e^{-\alpha x_R} + \alpha x_R \gamma(0) e^{-\alpha x_R} - \frac{2a}{\alpha} \gamma(0) \sinh(\alpha x_R) e^{-\alpha x_R}, \\ \gamma(p) &= \frac{r}{Da^2 p^2 - r} \Rightarrow \gamma(0) = -1, \quad \partial_p \gamma(p) = -\frac{2Drpa^2}{(Da^2 p^2 - r)^2} \Rightarrow \partial_p \gamma(p)|_{p \rightarrow 0} = 0, \\ \therefore \partial_p f_C(p, x_R)|_{p \rightarrow 0} &= -\alpha x_R e^{-\alpha x_R} + \frac{2a}{\alpha} \sinh(\alpha x_R) e^{-\alpha x_R}.\end{aligned}\quad (\text{C12})$$

Hence, the final expression of the average work is

$$\begin{aligned}\langle W \rangle &= e^{\alpha x_R} Q^2(0|x_R) \left[-\alpha x_R e^{-\alpha x_R} + \frac{2a}{\alpha} \sinh(\alpha x_R) e^{-\alpha x_R} \right] \\ &= \frac{a}{\alpha} [2 \sinh(\alpha x_R) - \alpha x_R].\end{aligned}\quad (\text{C13})$$

APPENDIX D: TRADE-OFF RELATION FOR LINEAR POTENTIAL

Here we discuss the trade-off plot for the linear trapping potential in detail. In Fig. 8, we have plotted $\langle t_{\text{ex}} \rangle|_{r=r_{\text{ex}}^*}$ (the solid curve) along with seven different sets of simulation (shown by the data points) of $\langle t_{\text{ex}} \rangle$ and the average work $\langle W \rangle$ in the joint phase space. Each set corresponds to a particular value of the potential strength a as shown in the figure. To ob-

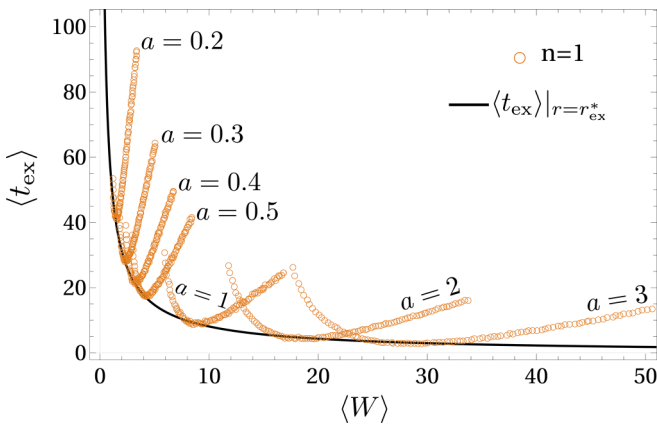


FIG. 8. Trade-off relation between excess time and work, i.e., plot of $\langle t_{\text{ex}} \rangle$ as a function of $\langle W \rangle$ for the $n = 1$ case. The solid curve denotes the minimum excess time $\langle t_{\text{ex}} \rangle|_{r=r_{\text{ex}}^*}$ for a given work, derived for $n = 1$. Data points are obtained from the simulation with various potential strengths a and reset rates r .

tain each of these sets we have varied the resetting rate in the range $\{0.005, 0.1\}$ and computed $\langle t_{\text{ex}} \rangle$ and $\langle W \rangle$, respectively, from Eqs. (19) and (21). As expected, all the data points stay above the lower bound depicted by the solid line. Only when the resetting rate becomes the optimal one r_{ex}^* in each case does the data fall onto the black solid line. We have performed similar simulations for other potentials and constructed an extended trade-off plot in Fig. 5.

APPENDIX E: CALCULATION OF MEAN FPT AND AVERAGE WORK FOR THE SHARP RESETTING PROTOCOL

Consider a Brownian particle freely diffusing in one-dimensional space. The particle can reach the target at a random time, say T , starting from an initial position x_0 . However, resetting can occur before the particle finds the target, resulting in resetting time $R < T$. In this case, the particle undergoes a return phase to the initial coordinate assisted by an external potential $U(x)$. Note that both T and R can be sampled from arbitrary distribution. Let x be the position of the particle when the reset phase starts and $\tau(x)$ be the mean time required to reach the resetting position x_R for the first time during the return phase. The mean global FPT to reach the target located at the origin then follows from [52]

$$\langle t_G \rangle = \frac{\langle \min(T, R) \rangle}{P(T < R)} + \frac{\int_0^\infty dt f_R(t) \int dx \tau(x) G_0(x, t|x_0, 0)}{P(T < R)}, \quad (\text{E1})$$

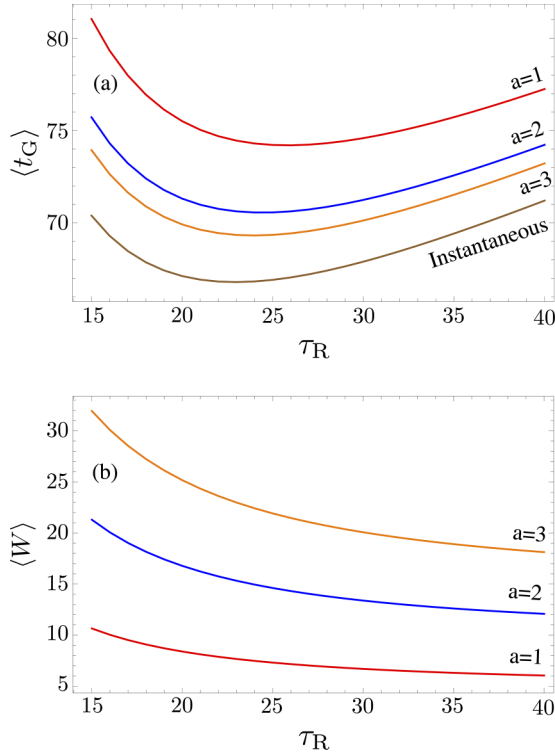


FIG. 9. Numerical results for the sharp resetting protocol. Plots for (a) $\langle t_G \rangle$ and (b) $\langle W \rangle$ as a function of τ_R for various values of a with the parameters $x_0 = x_R = 5$ and $D = D_R = 0.5$.

where $f_R(t)$ is the probability density function of the resetting time. For example, in the case of stochastic resetting, $f_R(t) = re^{-rt}$, and for sharp resetting, $f_R(t) = \delta(t - \tau_R)$. The propagator $G_0(x, t|x_0, 0)$ in Eq. (E1) is the conditional probability density to find the particle at position x at time t given that it started at x_0 at time $t = 0$, but in the presence of the target [63]

$$G_0(x, t|x_0, 0) = \frac{1}{\sqrt{4\pi Dt}} \left[e^{-\frac{(x-x_0)^2}{4Dt}} - e^{-\frac{(x+x_0)^2}{4Dt}} \right]. \quad (\text{E2})$$

Finally, for a simple Brownian particle, the mean reaching time $\tau(x)$ under the linear potential $U(x) = a|x - x_R|$ is given by

$$\tau(x) = -\partial_p Q_R(p|x)|_{p \rightarrow 0} = \frac{|x|}{a}. \quad (\text{E3})$$

Plugging all these expressions together into Eq. (E1) does not yield a closed expression; hence, we evaluate $\langle t_G \rangle$ numerically. The result is plotted in Fig. 9(a).

Similar to the mean first passage time, one can construct a renewal equation for the work by noting that it depends only on the number of times the particle undergoes a reset phase. Following the method presented in Ref. [52], one can then write a renewal equation for the work as

$$\begin{aligned} W &= 0 & \text{if } T < R, \\ &= U(x) + W' & \text{if } R \leq T, \end{aligned} \quad (\text{E4})$$

where W' is an independent and identically distributed copy of W which again has the possibilities to accumulate zero or a finite quantity. The above expression (E4) can be rewritten as

$$W = I(R \leq T)[U(x) + W'], \quad (\text{E5})$$

where $I(R \leq T)$ is an indicator function which takes value 1 if $R \leq T$ with probability $P(R \leq T)$ and is zero otherwise. Taking expectations on the both sides of Eq. (E5), we have

$$\begin{aligned} \langle W \rangle &= \langle I(R \leq T)[U(x) + W'] \rangle \\ &= \langle I(R \leq T)U(x) \rangle + P(R \leq T)\langle W' \rangle, \end{aligned} \quad (\text{E6})$$

where in the last equality we have considered the fact that W' is independent of W and $\langle I(R \leq T) \rangle = P(R \leq T)$. Finally, $\langle W \rangle = \langle W' \rangle$, since W' is an independent and identically distributed copy of W . Therefore, a simple rearrangement leads to

$$\langle W \rangle = \frac{\langle I(R \leq T)U(x) \rangle}{P(T < R)}, \quad (\text{E7})$$

which can be computed as shown in Ref. [52]. Following this, one finds

$$\langle W \rangle = \frac{\int_0^\infty dt f_R(t) \int dx U(x) G_0(x, t|x_0, 0)}{P(T < R)}. \quad (\text{E8})$$

For sharp resetting, we have calculated Eq. (E8) numerically. The result is plotted in Fig. 9(b). Since τ_R represents the time for the diffusion phase, higher values of τ_R imply lower numbers of the reset phase and, hence, lower average work. We finally make a note that Eq. (E8) is a very general expression that holds for arbitrary resetting time density, potential, and underlying search processes (and not limited to diffusion).

[1] R. Landauer, Irreversibility and heat generation in the computing process, *IBM J. Res. Dev.* **5**, 183 (1961).
 [2] J. M. R. Parrondo, J. M. Horowitz, and T. Sagawa, Thermodynamics of information, *Nat. Phys.* **11**, 131 (2015).
 [3] G. Diana, G. B. Bagci, and M. Esposito, Finite-time erasing of information stored in fermionic bits, *Phys. Rev. E* **87**, 012111 (2013).
 [4] A. B. Boyd, A. Patra, C. Jarzynski, and J. P. Crutchfield, Shortcuts to thermodynamic computing: The cost of fast and faithful erasure, *J. Stat. Phys.* **187**, 17 (2022).

[5] T. Schmiedl and U. Seifert, Optimal finite-time processes in stochastic thermodynamics, *Phys. Rev. Lett.* **98**, 108301 (2007).
 [6] K. Proesmans, J. Ehrich, and J. Bechhoefer, Finite-time Landauer principle, *Phys. Rev. Lett.* **125**, 100602 (2020).
 [7] K. Proesmans, J. Ehrich, and J. Bechhoefer, Optimal finite-time bit erasure under full control, *Phys. Rev. E* **102**, 032105 (2020).
 [8] A. Bérut, A. Arakelyan, A. Petrosyan, S. Ciliberto, R. Dillenschneider, and E. Lutz, Experimental verification of Landauer's principle linking information and thermodynamics, *Nature (London)* **483**, 187 (2012).

- [9] Y. Jun, M. Gavrilo, and J. Bechhoefer, High-precision test of Landauer's principle in a feedback trap, *Phys. Rev. Lett.* **113**, 190601 (2014).
- [10] Y.-Z. Zhen, D. Egloff, K. Modi, and O. Dahlsten, Universal bound on energy cost of bit reset in finite time, *Phys. Rev. Lett.* **127**, 190602 (2021).
- [11] J. S. Lee, S. Lee, H. Kwon, and H. Park, Speed limit for a highly irreversible process and tight finite-time Landauer's bound, *Phys. Rev. Lett.* **129**, 120603 (2022).
- [12] N. Shiraishi, K. Saito, and H. Tasaki, Universal trade-off relation between power and efficiency for heat engines, *Phys. Rev. Lett.* **117**, 190601 (2016).
- [13] J. S. Lee, J.-M. Park, H.-M. Chun, J. Um, and H. Park, Exactly solvable two-terminal heat engine with asymmetric Onsager coefficients: Origin of the power-efficiency bound, *Phys. Rev. E* **101**, 052132 (2020).
- [14] A. C. Barato and U. Seifert, Thermodynamic uncertainty relation for biomolecular processes, *Phys. Rev. Lett.* **114**, 158101 (2015).
- [15] A. Dechant and S.-i. Sasa, Fluctuation-response inequality out of equilibrium, *Proc. Natl. Acad. Sci. USA* **117**, 6430 (2020).
- [16] J. M. Horowitz and T. R. Gingrich, Thermodynamic uncertainty relations constrain non-equilibrium fluctuations, *Nat. Phys.* **16**, 15 (2020).
- [17] Y. Hasegawa and T. V. Vu, Fluctuation theorem uncertainty relation, *Phys. Rev. Lett.* **123**, 110602 (2019).
- [18] J. S. Lee, J.-M. Park, and H. Park, Universal form of thermodynamic uncertainty relation for Langevin dynamics, *Phys. Rev. E* **104**, L052102 (2021).
- [19] N. Shiraishi, K. Funo, and K. Saito, Speed limit for classical stochastic processes, *Phys. Rev. Lett.* **121**, 070601 (2018).
- [20] G. Falasco and M. Esposito, Dissipation-time uncertainty relation, *Phys. Rev. Lett.* **125**, 120604 (2020).
- [21] S. Ito and A. Dechant, Stochastic time evolution, information geometry, and the Cramér-Rao bound, *Phys. Rev. X* **10**, 021056 (2020).
- [22] J. S. Lee, J. M. Park, and H. Park, Thermodynamic uncertainty relation for underdamped Langevin systems driven by a velocity-dependent force, *Phys. Rev. E* **100**, 062132 (2019).
- [23] M. R. Evans and S. N. Majumdar, Diffusion with stochastic resetting, *Phys. Rev. Lett.* **106**, 160601 (2011).
- [24] S. Gupta, S. N. Majumdar, and G. Schehr, Fluctuating interfaces subject to stochastic resetting, *Phys. Rev. Lett.* **112**, 220601 (2014).
- [25] M. R. Evans, S. N. Majumdar, and G. Schehr, Stochastic resetting and applications, *J. Phys. A: Math. Theor.* **53**, 193001 (2020).
- [26] S. N. Majumdar, S. Sabhapandit, and G. Schehr, Dynamical transition in the temporal relaxation of stochastic processes under resetting, *Phys. Rev. E* **91**, 052131 (2015).
- [27] S. Eule and J. J. Metzger, Non-equilibrium steady states of stochastic processes with intermittent resetting, *New J. Phys.* **18**, 033006 (2016).
- [28] A. Pal, Diffusion in a potential landscape with stochastic resetting, *Phys. Rev. E* **91**, 012113 (2015).
- [29] V. Méndez and D. Campos, Characterization of stationary states in random walks with stochastic resetting, *Phys. Rev. E* **93**, 022106 (2016).
- [30] U. Basu, A. Kundu, and A. Pal, Symmetric exclusion process under stochastic resetting, *Phys. Rev. E* **100**, 032136 (2019).
- [31] S. Reuveni, Optimal stochastic restart renders fluctuations in first passage times universal, *Phys. Rev. Lett.* **116**, 170601 (2016).
- [32] A. Pal and S. Reuveni, First passage under restart, *Phys. Rev. Lett.* **118**, 030603 (2017).
- [33] A. Pal, I. Eliazar, and S. Reuveni, First passage under restart with branching, *Phys. Rev. Lett.* **122**, 020602 (2019).
- [34] Ł. Kuśmierz, S. N. Majumdar, S. Sabhapandit, and G. Schehr, First order transition for the optimal search time of Lévy flights with resetting, *Phys. Rev. Lett.* **113**, 220602 (2014).
- [35] A. Chechkin and I. M. Sokolov, Random search with resetting: A unified renewal approach, *Phys. Rev. Lett.* **121**, 050601 (2018).
- [36] S. Belan, Restart could optimize the probability of success in a Bernoulli trial, *Phys. Rev. Lett.* **120**, 080601 (2018).
- [37] R. Bar-Ziv, T. Tlusty, and A. Libchaber, Protein-DNA computation by stochastic assembly cascade, *Proc. Natl. Acad. Sci. USA* **99**, 11589 (2002).
- [38] A. Murugan, D. A. Huse, and S. Leibler, Speed, dissipation, and error in kinetic proofreading, *Proc. Natl. Acad. Sci. USA* **109**, 12034 (2012).
- [39] H. Bhaskaran and R. Russell, Kinetic redistribution of native and misfolded RNAs by a DEAD-box chaperone, *Nature (London)* **449**, 1014 (2007).
- [40] C. Hyeon and D. Thirumalai, Generalized iterative annealing model for the action of RNA chaperones, *J. Chem. Phys.* **139**, 121924 (2013).
- [41] S. Chakrabarti, C. Hyeon, X. Ye, and D. Thirumalai, Molecular chaperones maximize the native state yield on biological times by driving substrates out of equilibrium, *Proc. Natl. Acad. Sci. USA* **114**, E10919 (2017).
- [42] S. Jain, D. Boyer, A. Pal, and L. Dagdug, Fick-Jacobs description and first passage dynamics for diffusion in a channel under stochastic resetting, *J. Chem. Phys.* **158**, 054113 (2023).
- [43] S. Reuveni, M. Urbakh, and J. Klafter, Role of substrate unbinding in Michaelis-Menten enzymatic reactions, *Proc. Natl. Acad. Sci. USA* **111**, 4391 (2014).
- [44] J. Fuchs, S. Goldt and U. Seifert, Stochastic thermodynamics of resetting, *Europhys. Lett.* **113**, 60009 (2016).
- [45] A. Pal and S. Rahav, Integral fluctuation theorems for stochastic resetting systems, *Phys. Rev. E* **96**, 062135 (2017).
- [46] F. Mori, K. S. Olsen, and S. Krishnamurthy, Entropy production of resetting processes, *Phys. Rev. Res.* **5**, 023103 (2023).
- [47] A. Pal, Ł. Kuśmierz, and S. Reuveni, Invariants of motion with stochastic resetting and space-time coupled returns, *New J. Phys.* **21**, 113024 (2019).
- [48] A. Pal, Ł. Kuśmierz, and S. Reuveni, Time-dependent density of diffusion with stochastic resetting is invariant to return speed, *Phys. Rev. E* **100**, 040101(R) (2019).
- [49] A. Maso-Puigdellosas, D. Campos, and V. Mendez, Transport properties of random walks under stochastic noninstantaneous resetting, *Phys. Rev. E* **100**, 042104 (2019).
- [50] A. S. Bodrova and I. M. Sokolov, Resetting processes with noninstantaneous return, *Phys. Rev. E* **101**, 052130 (2020).
- [51] A. S. Bodrova and I. M. Sokolov, Brownian motion under noninstantaneous resetting in higher dimensions, *Phys. Rev. E* **102**, 032129 (2020).
- [52] A. Pal, Ł. Kuśmierz, and S. Reuveni, Search with home returns provides advantage under high uncertainty, *Phys. Rev. Res.* **2**, 043174 (2020).

- [53] D. Gupta, C. A. Plata, A. Kundu, and A. Pal, Stochastic resetting with stochastic returns using external trap, *J. Phys. A: Math. Theor.* **54**, 025003 (2020).
- [54] D. Gupta, C. A. Plata, A. Pal, and A. Kundu, Resetting with stochastic return through linear confining potential, *J. Stat. Mech.* (2021) 043202.
- [55] Despite the possibility of the particle touching the target in the reset phase, the reset dynamics continues prior to the reset point in our model. This likelihood is low, though, as the reset potential induces a directional motion of the particle to the reset point, away from the target. In the limit of a strong potential, this likelihood becomes negligible.
- [56] S. N. Majumdar, Brownian functionals in physics and computer science, *Curr. Sci.* **89**, 2076 (2005).
- [57] P. Singh and A. Pal, First-passage Brownian functionals with stochastic resetting, *J. Phys. A: Math. Theor.* **55**, 234001 (2022).
- [58] D. Gupta, C. A. Plata, and A. Pal, Work fluctuations and Jarzynski equality in stochastic resetting, *Phys. Rev. Lett.* **124**, 110608 (2020).
- [59] D. Gupta and C. A. Plata, Work fluctuations for diffusion dynamics submitted to stochastic return, *New J. Phys.* **24**, 113034 (2022).
- [60] A. Pal, A. Kundu, and M. R. Evans, Diffusion under time-dependent resetting, *J. Phys. A: Math Theor.* **49**, 225001 (2016).
- [61] O. Tal-Friedman, A. Pal, A. Sekhon, S. Reuveni, and Y. Roichman, Experimental realization of diffusion with stochastic resetting, *J. Phys. Chem. Lett.* **11**, 7350 (2020).
- [62] B. Besga, A. Bovon, A. Petrosyan, S. N. Majumdar, and S. Ciliberto, Optimal mean first passage time for a Brownian searcher subjected to resetting: Experimental and theoretical results, *Phys. Rev. Res.* **2**, 032029(R) (2020).
- [63] S. Redner, *A Guide to First-Passage Processes* (Cambridge University, Cambridge, England, 2007).